NeuroImage: Clinical 25 (2020) 102132

Contents lists available at ScienceDirect

NeuroImage: Clinical

journal homepage: www.elsevier.com/locate/ynicl

Spatiotemporal EEG microstate analysis in drug-free patients with Parkinson's disease

Chunguang Chu[a,#], Xing Wang[b,#], Lihui Cai[a], Lei Zhang[b], Jiang Wang[a], Chen Liu[a,*], Xiaodong Zhu[b,*]

[a] School of Electrical and Information Engineering, Tianjin University, Tianjin, 300072, PR China
[b] Department of Neurology, Tianjin Medical University General Hospital, Tianjin, 300052, PR China

A B S T R A C T

The clinical diagnosis of Parkinson's disease (PD) is very difficult, especially in the early stage of the disease, because there is no physiological indicator that can be referenced. Drug-free patients with early PD are characterized by clinical symptoms such as impaired motor function and cognitive decline, which was caused by the dysfunction of brain's dynamic activities. The indicators of brain dysfunction in patients with PD at an early unmedicated condition may provide a valuable basis for the diagnosis of early PD and later treatment. In order to find the spatiotemporal characteristic markers of brain dysfunction in PD, the resting-state EEG microstate analysis is used to explore the transient state of the whole brain of 23 drug-free patients with PD on the sub-second timescale compared to 23 healthy controls. EEG microstates reflect a transiently stable brain topological structure with spatiotemporal characteristics, and the spatial characteristic microstate classes and temporal parameters provide insight into the brain's functional activities in PD patients. The further exploration was to explore the relation between temporal microstate parameters and significant clinical symptoms to determine whether these parameters could be used as a basis for clinically assisted diagnosis. Therefore, we used a general linear model (GLM) to explore the relevance of microstate parameters to clinical scales and multiple patient attributes, and the Wilcoxon rank sum test was used to quantify the linear relation between influencing factors and microstate parameters. Results of microstate analysis revealed that there was an unique spatial microstate different from healthy controls in PD, and several other typical microstates had significant differences compared with the normal control group, and these differences were reflected in the microstate parameters, such as longer durations and more occurrences of one class of microstates in PD compared with healthy controls. Furthermore, correlation analysis showed that there was a significant correlation between multiple microstate classes' parameters and significant clinical symptoms, including impaired motor function and cognitive decline. These results indicate that we have found multiple quantifiable feature tags that reflect brain dysfunction in the early stage of PD. Importantly, such temporal dynamics in microstates are correlated with clinical scales which represent the motor function and recognize level. The obtained results may deepen our understanding of the brain dysfunction caused by PD, and obtain some quantifiable signatures to provide an auxiliary reference for the early diagnosis of PD.

1. Introduction

Parkinson's disease (PD) is a degenerative neurological disorder of certain nerve cells in the part of the brain which produces dopamine (Rigas et al., 2009), and it is characterized by movement symptoms such as resting tremor, bradykinesia, rigidity and postural instability (Dickson, 2017). PD generally occurs in middle and old age (after 50 years old), and its average age of onset is about 60 years old. It is a long-term disease and progresses gradually for several years. This causes the patients to lose self-care ability and even leads to disability.

In terms of cardinal manifestations, bradykinesia and resting tremor (RT) are two kinds of the most frequent manifestations of PD (Berardelli, 2001), and RT is the second most common motor symptom of PD, after bradykinesia (Rigas et al., 2009; Jankovic, 2008; Schwingenschuh et al., 2010). In terms of pathophysiological substrate, PD is characterized by dopamine depletion in the striatum, which disrupts corticostriatal processing and explains clinical symptoms such as bradykinesia and rigidity. In addition to movement symptoms such as tremor and tardiness, PD patients may also have non-movement symptoms such as depression, anxiety, sleep disorders and cognitive disorders.

At the early stage, the clinical diagnosis of PD is accomplished in combination with clinical symptoms, clinical scale scores, neuroimaging data, and other supporting criteria, such as response to dopamine therapy (Serrano et al., 2018). Accurate diagnosis of Parkinson's disease is always difficult because of the complex etiology and the variety of clinical symptoms, especially in the early stage of the disease (Serrano et al., 2018).

* Corresponding authors.
E-mail addresses: ccg_tina@tju.edu.cn (C. Chu), cdwangxing5118@126.com (X. Wang), clhfio@tju.edu.cn (L. Cai), 15522015351@163.com (L. Zhang), jiangwang@tju.edu.cn (J. Wang), liuchen715@tju.edu.cn (C. Liu), zxd3516@tmu.edu.cn (X. Zhu).
Joint first authors.

https://doi.org/10.1016/j.nicl.2019.102132
Received 22 July 2019; Received in revised form 4 December 2019; Accepted 13 December 2019
Available online 20 December 2019

In order to assist in the accurate clinical diagnosis of early PD and avoid the diagnosis of PD through the detection of patients' response to dopamine due to the complex and unclear initial symptoms of PD, it is necessary to explore the status markers that are difficult to identify in early PD. Therefore, the search for valuable neurophysiological identification of early PD is an urgent problem to be solved, and the found significant status characteristics of early PD will be an excellent auxiliary means to improve the certainty of clinical diagnosis (VallsSolé and Valldeoriola, 2002).

In the pathology of Parkinson's disease, the dynamic changes in the brain's activity play an important role (Serrano et al., 2018) which can be assessed on different time scales and with different types of data: functional magnetic resonance imaging (fMRI) with high spatial resolution can characterize slower brain dynamics; quantifying electroencephalography (EEG) variations in both time domain and frequency domain is a basic way to characterize the state markers of several neurodegenerative diseases, such as PD, or some neuropsychiatric disorders as major depressive disorder and schizophrenia (Gandal et al., 2012; Han et al., 2013). It is worth noting that Kannan et al (2012;2011) have performed very high fidelity 2D and 3D simulations for accurately and efficiently predicting and quantifying local and global injuries for organs like the brain and the lung. They were able to (i) noninvasively 'numerically penetrating' the tissues and (ii) reconstruct the optical properties the presence of water, oxygenated and de-oxygenated blood. These numerical noninvasive measurements are then used to predict the extent and severity of the organ hemorrhage/injury. What's more, compared with other expensive invasive surgery or imaging technologies, such as electrocorticography (ECoG) and fMRI, EEG recording system, as a cheaper and more mobile medical device, has been used widely to analysis the dynamic changes in the brain's activity, and it is expected to become a common tool for the diagnosis of PD in the early stage of the disease in the future (Chu et al., 2018).

EEG microstate analysis with inherent high temporal resolution and high test-retest reliability can study sub-second dynamic changes in brain activity (Schumacher et al., 2019). EEG microstates are defined as global patterns of scalp potential topographies which using multichannel EEG arrays that dynamically vary over time in an organized manner (Milz et al., 2015). EEG microstates have been studied extensively in wakefulness, where four standard classes of EEG-microstate maps have been repeatedly identified in a large number of studies on healthy subjects of all ages at rest (Schlegel et al., 2012; Koenig et al., 2002). The morphological changes of brain electric field are nonlinear and discontinuous. A given structure of brain electric field tends to maintain a quasi-stable state for a sub-second time period before rapidly transforming into another different structure. These periods of quasi-stable field structure were called microstates and were suggested to reflect basic steps in brain information processing in spontaneous and event-related studies (Brandeis and Lehmann, 1989; Lehmann et al., 1987; Koenig et al., 1998). Many related studies have demonstrated that the characteristics caused by dynamic changes in brain activity, such as personality types (Schlegel et al., 2012) and behavioral states (Lehmann et al., 2010), as well as the disorders caused by abnormal brain activity, such as neuropsychiatric disorders (Lehmann et al., 2005; Mitsuru et al., 2011; Khanna et al., 2015), are the drivers of changes in time series of EEG microstates. Consequently, the presence of particular microstates that reflect different brain activities and abnormalities in their inherent characteristics (including frequency or duration, etc.) can be considered as quantifiable characteristic state markers of different neuropsychiatric and neurological disorders (Serrano et al., 2018). Besides, the broader literature suggests that dynamic brain activities characterized by flexibility in brain activity and temporal variability are associated with cognitive function (Schumacher et al., 2019; Deco et al., 2011; Garrett et al., 2013; Zalesky et al., 2014).

Thus, EEG microstate analysis is conducted in this work, aiming to explore the pathological characteristics of brain activity in early-stage PD by revealing the differences of dynamic brain activities between the healthy subjects and drug-free patients with the manifestations of tremor or bradykinesia in the early stage of PD. And these quantifiable pathological characteristics can be used as auxiliary diagnostic tools to help clinicians accurately diagnose early PD.

Moreover, state markers to characterize the feature of PD patients with typical movement symptoms are expected to be extracted from the EEG-microstate approach. What's more, we explored the association between microstate features and clinical scale scores to explain the relation between brain dynamics changes and both movement disorders and cognitive impairments caused by PD pathology.

2. Materials and methods

2.1. Participants

23 patients treated in the department of psychiatry of Tianjin Medical University General Hospital were included in the study (15 female: age range of 60–74, mean age of 67 years old; 8 male: age range of 65–75, mean age of 68 years old).

Among all the patients, the first symptom of 9 patients was bradykinesia, and the other 14 was resting tremor. All of them had been diagnosed as primary PD with 3.2 ± 2.5 years' disease duration, and all patients had been off medication for more than 12 h in order to collect EEG data in the absence of pharmacodynamic effects (means drug-free). None of the patients had head tremor. In addition, 23 age-matched and gender-matched healthy participants (12 female: age range of 60–70, mean age of 65 years old; 11 male: age range of 60–74, mean age of 66 years old) with no history of neurological or psychiatric illness were recruited as a control group. Table 1 describes the detailed information of included patients.

2.2. Acquisition protocol

A series of EEG time series were recorded while all subjects lay comfortably in a quiet semi-dark room and stayed awake with their eyes closed. EEG signals were collected between 9 a.m. and 11 a.m.. EEG activities were recorded at 19 positions of the brain. Besides, eye movements were recorded with four EOG channels (positioned at the eye's infra- and supraorbitally and canthi bilaterally on the left). The impedance of all the channels kept below 5kΩ.

All patients received a detailed behavioral and neuropsychiatric assessment. The evaluation scales used in the present study are the third part of Movement Disorder Society-Sponsored Revision of the Unified Parkinson's Disease Rating Scale (MDS-UPDRS) and Montreal Cognitive Assessment (MoCA). The third part of MDS-UPDRS and MoCA can be used as a quantitative criterion to assess patients with dyskinesia and cognitive impairment, respectively (Wang et al., 2014; Schwingenschuh et al., 2010). The local ethics committee approved the study. The purpose and research significance of this data were explained to all participants, and written informed consent was obtained.

2.3. Analysis materials

Resting EEG data were recorded from 19 Ag/AgCl scalp electrodes (active electrodes, SYMTOP, Beijing, China) represented to 19 positions that were placed according to the 10–20 system as shown in Fig. 1, here, A1 and A2, linking the both earlobes, used as the references, and these 19 Ag/AgCl scalp electrodes are linked to 19 data channels. An UEA-BZ amplifier (SYMTOP, Beijing, China) was linked to the 19 data channels to amplify and digitize the EEG data. The processing of EEG acquisition was carried out by Study Rome software. The EEG signal preprocessing was performed by the EEGLab toolbox in MATLAB software (MathWorks Inc., Natick MA, United States). EEG microstate analyses were handed by Cartool (the Key Institute for Brain-Mind Research, Zurich, Switzerland). Statistical analyses were performed by

Table 1
Description of the patients with PD and healthy controls included in the study.

PD Group							HC Group			
	Gender	Age	D. D. (year)	Starting Symptoms	The Third Part of MDS-UPDRS	MoCA		Gender	Age	MoCA
1	Female	68	1	Tremor	11	27	1	Male	66	29
2	Female	62	6	Tremor	14	27	2	Female	64	28
3	Female	65	3	Tremor	11	29	3	Female	67	27
4	Male	67	6	Tremor	13	27	4	Female	60	30
5	Female	65	1	Tremor	10	27	5	Male	68	29
6	Female	65	1	Tremor	11	19	6	Male	65	28
7	Male	75	4	Tremor	48	21	7	Female	66	27
8	Female	71	1	Tremor	13	25	8	Male	62	27
9	Female	74	1	Tremor	9	25	9	Male	65	28
10	Female	68	3	Tremor	11	30	10	Female	67	26
11	Female	60	2	Tremor	23	26	11	Female	65	26
12	Female	66	0.25	Tremor	11	29	12	Male	72	28
13	Male	69	4	Tremor	18	27	13	Male	69	29
14	Female	65	9	Tremor	24	29	14	Female	63	29
15	Male	65	3	Bradykinesia	13	30	15	Female	61	28
16	Male	66	0.5	Bradykinesia	24	27	16	Male	63	27
17	Female	73	2	Bradykinesia	27	28	17	Male	74	26
18	Male	63	1	Bradykinesia	16	27	18	Male	66	28
19	Female	67	7	Bradykinesia	18	26	19	Female	69	27
20	Female	72	4	Bradykinesia	39	26	20	Male	61	30
21	Female	70	1	Bradykinesia	16	29	21	Female	60	29
22	Male	68	2	Bradykinesia	34	23	22	Female	70	28
23	Male	66	1	Bradykinesia	11	22	23	Female	64	30

PD, drug-free patients with Parkinson's Disease; HC, healthy controls; D. D., disease duration; MDS-UPDRS, Movement Disorder Society-Sponsored Revision of the Unified Parkinson's Disease Rating Scale; MoCA, Montreal Cognitive Assessment.

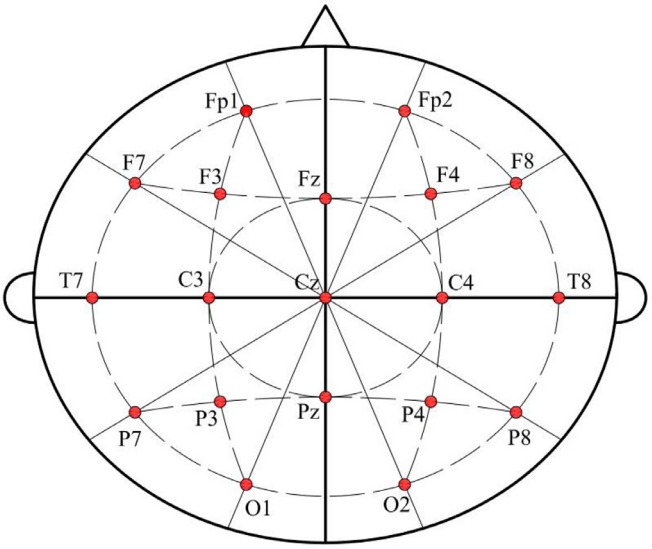

Fig. 1. Electroencephalography (EEG) electrode positions on the brain.

MATLAB software (MathWorks Inc., Natick MA, United States) and SPSS 25.0 software (IBM Inc., Chicago, IL, United States).

2.4. EEG preprocessing

The sampling frequency of the EEG data was 500 Hz. Each participant's EEG data was monitored lasting for 10 to 20 min. Resting EEG data were preprocessed by MATLAB software. All of the EEG data were carefully checked for artifacts (body movements, eyes movements, technical artifacts, muscle activity). The epochs of EEG that were contaminated due to the presence of artifacts were rejected. Continuous EEG recordings for a total of 3 min of each subject were retained for microstate analyses. Ocular correction Independent Component Analysis (ICA) were applied on the continuous EEG signal for each channel by the fast ICA algorithm and then each EEG epochs was processed by a 2–20 Hz band-pass Finite Impulse Response (FIR) filter to eliminate the interference of high frequency noises.

2.5. EEG microstate analysis

The pre-processed data were imported into CARTOOL for the following microstate analysis, in order to detect EEG microstates and compute the characterization. The Global Field Power (GFP) is a measure of the strength of a scalp potential and is based on potential differences between all electrodes at each sampling point, leading to a scalar value of field strength for each sampling point (Skrandies, 1989).

$$GFP = \sqrt{\frac{\sum_{i=1}^{n} u_i^2}{n}} \quad (1)$$

Here, i denotes each electrode, n represents the number of electrodes (here is 19) and u denotes the measured voltage of each channel. High GFP is in connection with a stable EEG topography around its peak (Menendez and Micah, 2004). Since the signal-to-noise ratio of EEG signals is the highest at the peak of GFP, the momentary voltage amplitude values of all electrodes at the time point of GFP peaks were selected for clustering analysis. For microstate segmentation, a clustering algorithm called modified K-means algorithm in literature (Murray et al., 2008) was used to compute EEG microstates.

Fig. 2 shows the process of EEG microstate analysis. We used the Cartool software to perform the microstate analysis in three steps. In the first step, the global field power time series (GFP, blue line) was computed as the spatial standard deviation of the EEG topography at each given time. At local GFP maxima (red dots), the spatial configuration of the EEG was considered stable and explains most of the variance of the time series that at the time point of the GFP maximum was marked green vertical line. The instantaneous EEG potential fields at the maximum value of GFP were referred to as maps in this work. In the second step, modified k-means clustering approach was performed on the scalp maps of each participant. Several studies that used the k-means clustering analysis and determined the optimal number of clusters by the cross-validation (CV) criterion demonstrate that the optimal number of classes within subjects was four (this is consistent with literature (Koenig et al., 1999; Britz et al., 2010; Brodbeck et al., 2012)). So we set the number of clusters from 2 to 6 and the optimum

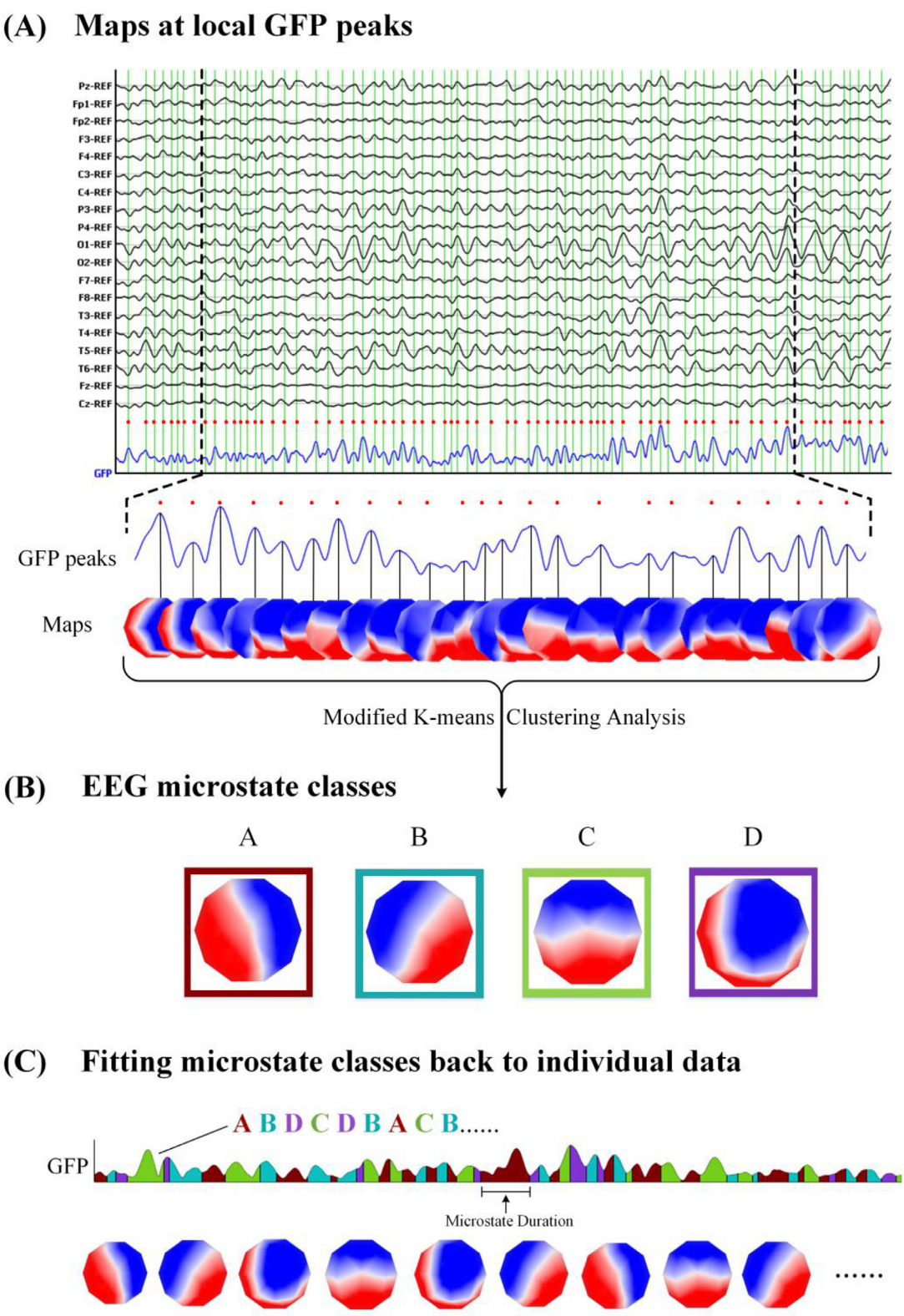

Fig. 2. Schematic diagram of the microstate analysis process: (A) A 2-second EEG is extracted from the spontaneous EEG. The GFP of each sampling point is calculated and all topographic maps at the local GFP maxima are obtained. (B) The improved K-means clustering analysis method is used to analyze the original topographic maps to obtain four optimal microstates classes. (C) Microstate temporal sequences are obtained by fitting four microstate classes back to complete EEG data.

set of classes was selected according to the maximum global explained variance (GEV), and then original momentary maps of both groups (PD group and the health group) were separately clustered into four microstate classes. Finally, the generated class-labeled group maps were used as templates to assign original individual successive EEG series of each subject to four microstate classes (A, B, C and D class which displayed in Fig. 2 for each group respectively).

The spatial correlation across the template maps between the groups

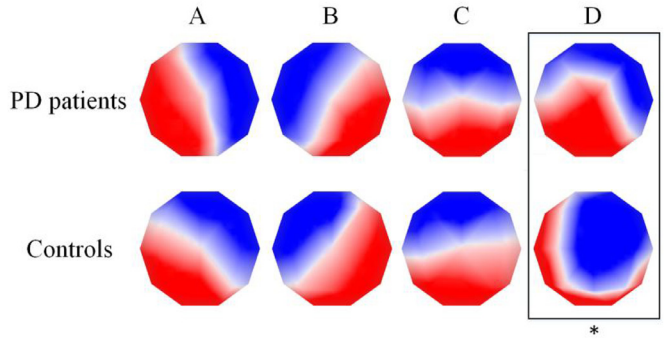

Fig. 3. Microstate classes of PD patients and healthy controls. There is a post-hoc test (implemented by TANOVA): significant statistical difference between PD patients and healthy controls is indicated by one asterisk ($p < 0.05$).

was analyzed with the scalp instantaneous topographic maps of each subject. In order to compare the differences of EEG microstates between PD and normal people, the following microstate parameters for each microstate segmentation class were calculated:

(a) Mean Microstate Duration (MMD): Mean length of microstate segments (in time frame) as shown in Fig. 1;
(b) Occurrence Per Second (OPS): Frequency of occurrence of the same microstate class across all analysis epochs;
(c) Ratio of Time Coverage (RTC): Time coverage percentage of each microstate class across all analysis epochs.

2.6. Statistical analysis

Each microstate characteristic parameter of PD and normal subjects was compared. The group differences of microstate parameters mentioned above between PD group and the control group were tested by Wilcoxon rank sum test separately. In the case of significant differences between the class of microstate and the group, the Wilcoxon rank sum test were followed up by the pairwise comparison afterwards (the least significant difference method) to further explore the differences between the groups. Generally, statistical significance is accepted with a p-value of rank sum test lower than 0.01 (Wang et al., 2015).

To test the differences of the microstate classes' topographies between the groups, Topographic ANalysis of VAriance (TANOVA, see literature (Koenig et al., 2011; Koenig and Pascualmarqui, 2009) for detail) was implemented. Statistical signifcant differences were assessed at $p \leq 0.01$ (Koenig et al., 2011; Koenig and Pascualmarqui, 2009).

As an exploratory analysis, in order to explore the correlations between clinical scales (included the third part of MDS-UPDRS and MoCA) and the microstate parameters of each microstate class in PD patients respectively, we need to consider the influences of gender, age, disease duration, and initial symptom simultaneously. Consequently, the general linear model (GLM) was used to analyze the correlation analysis under the action of multiple factors.

We assume that the experimental data for each microstate parameters of each microstate classes can be modeled by the GLM written as follows (the GLM represents k observations, including disease duration, age, gender, initial symptoms and clinical scales):

$$Y_i = \sum_{n=1}^{k} \beta_{ni} X_{ni} + \varepsilon_i \quad (2)$$

where Y is the experimental data for each microstate parameters of each microstate classes, i is the subscript of the microstate parameter, $i = 1, \cdots, m$, m is the total number of the microstate classes' microstate parameters, and it's also the number of the GLMs. X_{ni} is the independent variable matrix, for example, X_{1i} means a matrix of disease duration. β_{ni} is a coefficient vector which represents the response of microstate parameter i to the stimulus measured by independent variable n, and k is the number of independent variables. ε_i is the error vector. Each GLM characterizes the regression model of each microstate parameter under the influence of multivariate conditions, and there is a different regression model for each microstate parameter. The parameter estimation of the GLM was calculated by SPSS 25.0 software (IBM Inc., Chicago, IL, United States) and a p value < 0.05 was considered statistically significant.

Further more, in order to quantify the linear relationship, Spearman's correlations between clinical scales (included the third part of MDS-UPDRS and MoCA) and the microstate parameters of each microstate class were tested in PD patients respectively. Corrected FDR (false discovery rate) acted on $P-$ values for multiple comparisons. The significant Spearman's correlation between the microstate parameter and the clinical scales was accepted at $P < 0.05$.

3. Results

3.1. Microstate class spatial topographies

In order to explore the differences in microstate topographic maps between PD group and the control group, we used microstate analysis to analyze the original scalp EEG topography of each subject by group. According to the microstate segmentation templates of the both groups, we can find whether there is a significant difference in the clustering state between PD group and the control group.

Fig. 3 shows the microstate topographic classes of the PD group and the control group. In order to explore whether the four resting state EEG microstates' topographies differ in the two factors, Topographic ANalysis of VAriance (TANOVA) was applied to each microstate class in both groups to compare the microstates' topographies between the PD patients and healthy controls. There is a significant change in the resting EEG microstate class "D" topography ($p < 0.01$) and no differences ($p > 0.05$) are found in the other three microstate classes.

3.2. Microstate temporal characteristics

The four microstate classes totally accounted for 82.47% (S.D.: 5.23%) of the Global Explained Variance (GEV) across PD patients, and of 85.56% (S.D.: 4.58%) across the healthy controls. Microstate classes A to C of the both groups (shown in the Fig. 3) corresponded well to the canonical microstate classes A to C that have been reported in the literature (Van et al., 2010). Microstate class A indicates an upper left-bottom right orientation, class B indicates an upper right-bottom left orientation, class C indicates an anterior-posterior orientation. Microstate class D of the control group (shown in Fig. 3) is a kind of canonical microstate class which has been reported in the literature (Van et al., 2010), and it indicates a trend of increasing gradually from the front to the center to the maximum. Compared with the template topographic class of the control group, the PD group did not have a canonical microstate class D matching the control group.

On the contrary, microstate class D of the PD group (shown in Fig. 4) indicates a trend of increasing from the back to the center to the maximum. In addition, during the clustering analysis, when the template microstate class D which matched the one of the control group was selected as the mapping template to fit the scalp EEG of PD patients, the resulting value of GEV was very small, less than 1% (it indicates that this type of topographic map is almost nonexistent). Similarly, the template microstate class D of the PD group was rarely found in the control group. Therefore, the abnormality of microstate class D may serve as a state marker for drug-free PD patients with distinct movement dysfunction (bradykinesia or tremor).

The Wilcoxon rank sum test was used to analyze the statistically differences of the microstate parameters between PD group and control group at the individual level of participants. The differences between

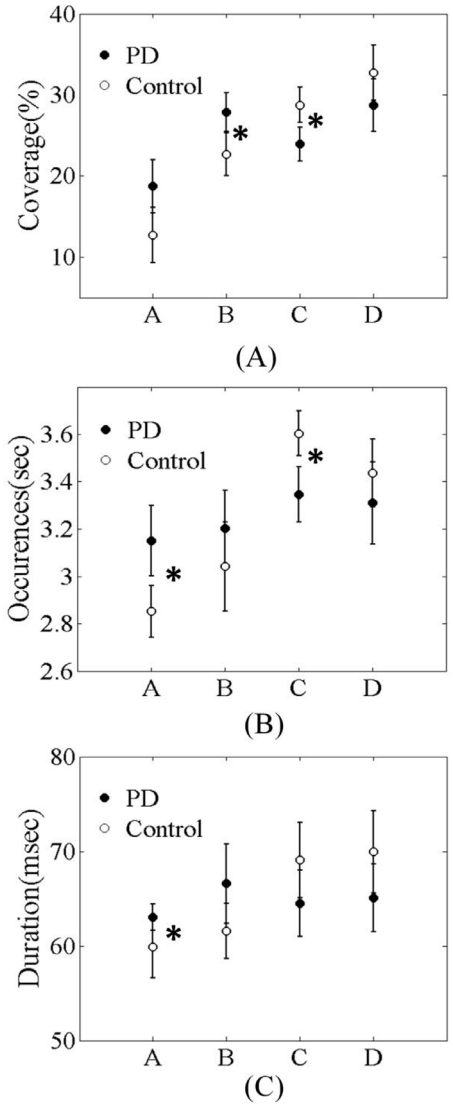

Fig. 4. Microstate characteristic statistics. The graphs display the coverage (RTC, (A)), occurrences (OPS, (B)) and duration (MMD, (C)) (from top to bottom) of the four microstate classes (A-D) in drug-free patients with PD (23 subjects; the mean of each characteristic is expressed as solid circle) and healthy controls (23 subjects; the mean of each characteristic is expressed as solid circle) with standard errors corresponding to the mean. Significant differences between groups are indicated by asterisks (* means $p < 0.01$).

groups with coverage (RTC), occurrence (OPS), and duration (MMD) for the four microstate classes are shown in Table 2 and Fig. 4.

As shown in Fig. 4, the Wilcoxon rank sum test indicated that mean MMD, OPS and RTC of microstates class A and class B in PD group are higher than those in the healthy control group, while these characteristic parameters of microstate class C and class D are decreased in PD group compared to healthy controls.

By comparing the differences between the groups of PD and HC, we can find significant differences in RTC, OPS and MMD. The RTC ranged between 12.73% and 32.73% for 4 microstate classes in both groups. The Wilcoxon rank sum test showed a significant more time coverage in microstate class B and less time coverage in microstate class C in PD patients than healthy controls ($p < 0.01$) (Fig. 4A, Table 2). The OPS varied from 2.85 to 3.60 maps/s for 4 microstate classes in both groups. According to the rank sum test, microstate class A was significantly more frequent in PD patients compared to healthy controls, and microstate class C was significantly less frequent ($p < 0.01$) (Fig. 4B, Table 2). The MMD covered from 59.88 ms to 69.93 ms for 4 microstate classes in both groups. The Wilcoxon rank sum test showed that the duration of microstate class A significantly increased ($p < 0.01$) (Fig. 4C, Table 2). These significant changes in microstate parameters may serve as a feature label for PD to further realize auxiliary diagnosis and personalized treatment.

Table 2
Microstate characteristic parameters and differences between-group comparisons.

	Parkinson's Disease (PD)				Healthy Controls (HC)				
	Mean	*(S.D.)*	Median	*(MAD)*	Mean	*(S.D.)*	Median	*(MAD)*	Rank sum test p-value
RTC (%)									
A	18.72	*(3.25)*	17.31	*(2.82)*	12.73	*(3.40)*	12.54	*(2.41)*	0.027
B	27.86	*(2.35)*	27.62	*(2.04)*	22.66	*(2.63)*	21.51	*(2.04)*	**<0.01**
C	23.90	*(2.07)*	24.27	*(1.68)*	28.75	*(2.19)*	27.57	*(1.68)*	**<0.01**
D	28.72	*(3.25)*	27.31	*(2.82)*	32.73	*(3.40)*	33.83	*(2.73)*	0.015
OPS									
A	3.14	*(0.15)*	3.14	*(0.11)*	2.85	*(0.11)*	2.84	*(0.09)*	**<0.01**
B	3.20	*(0.16)*	3.20	*(0.14)*	3.04	*(0.19)*	3.00	*(0.15)*	0.058
C	3.35	*(0.12)*	3.37	*(0.11)*	3.60	*(0.10)*	3.58	*(0.08)*	**<0.01**
D	3.31	*(0.17)*	3.30	*(0.14)*	3.44	*(0.14)*	3.40	*(0.12)*	0.090
MMD (ms)									
A	63.02	*(3.37)*	62.68	*(1.00)*	59.88	*(3.23)*	60.53	*(2.48)*	**<0.01**
B	66.57	*(4.20)*	66.30	*(3.33)*	61.57	*(2.93)*	60.59	*(2.28)*	0.031
C	64.47	*(3.49)*	64.45	*(2.80)*	69.06	*(3.97)*	68.96	*(3.06)*	0.012
D	65.08	*(3.58)*	63.26	*(2.96)*	69.93	*(4.31)*	68.12	*(3.89)*	0.017

Statistical significant differences were assessed at $p \leq 0.01$ and are marked in bold type.

3.3. Clinical correlations

3.3.1. Correlation between microstate parameters and comprehensive factors

The general linear model (GLM) was used to explore the clinical correlation between microstate parameters of each microstate class and the clinical comprehensive characteristics (including disease duration, age, gender, initial symptoms and clinical scales as shown in the Table 1). As shown in Fig. 5 and Table 3, the result shows that PD patients' clinical objective attributes (including disease duration, age, gender, and initial symptoms (tremor or bradykinesia)) are not significantly correlated with microstate parameters (such as the duration or frequency of a condition) with $P \geq 0.05$, and the microstate parameters of healthy controls are not significantly correlated with their age, gender or MoCA with $P \geq 0.05$, while there was a significant correlation between the scores of clinical scales and microstate parameters with $P < 0.05$.

Obviously, the clinical objective attributes of PD patients do not affect the negative correlation between OPS of microstate class A ($F = 5.46$, $\beta = -0.005$, $P = 0.03$) and the third part of the MDS-UPDRS in the PD patients, or the positive correlation between OPS of microstate class C ($F = 5.70$, $\beta = -0.016$, $P = 0.03$) and the MoCA in the PD patients, the same as the negative correlation between MMD of microstate class B ($F = 4.76$, $\beta = -0.072$, $P = 0.04$) and the MoCA in the PD patients under the action of multiple influencing factors.

After correcting for the confounding effects of disease duration, age, gender, initial symptoms, we have calculated the linear regression between the clinical scales and microstate parameters by GLM to explore the association between the microstate parameters and the clinical scales' scores. As shown in Table 4, there is a significant negative correlation between OPS of microstate class A and the third part of MDS-UPDRS in PD patients ($R^2 = 0.469$, $\beta = -0.380$, $P = 0.034$), and a significant positive correlation between OPS of microstate class C and the MoCA in PD patients ($R^2 = 0.520$, $\beta = 0.500$, $P = 0.015$). What's more, the significant negative correlation between MMD of microstate class B

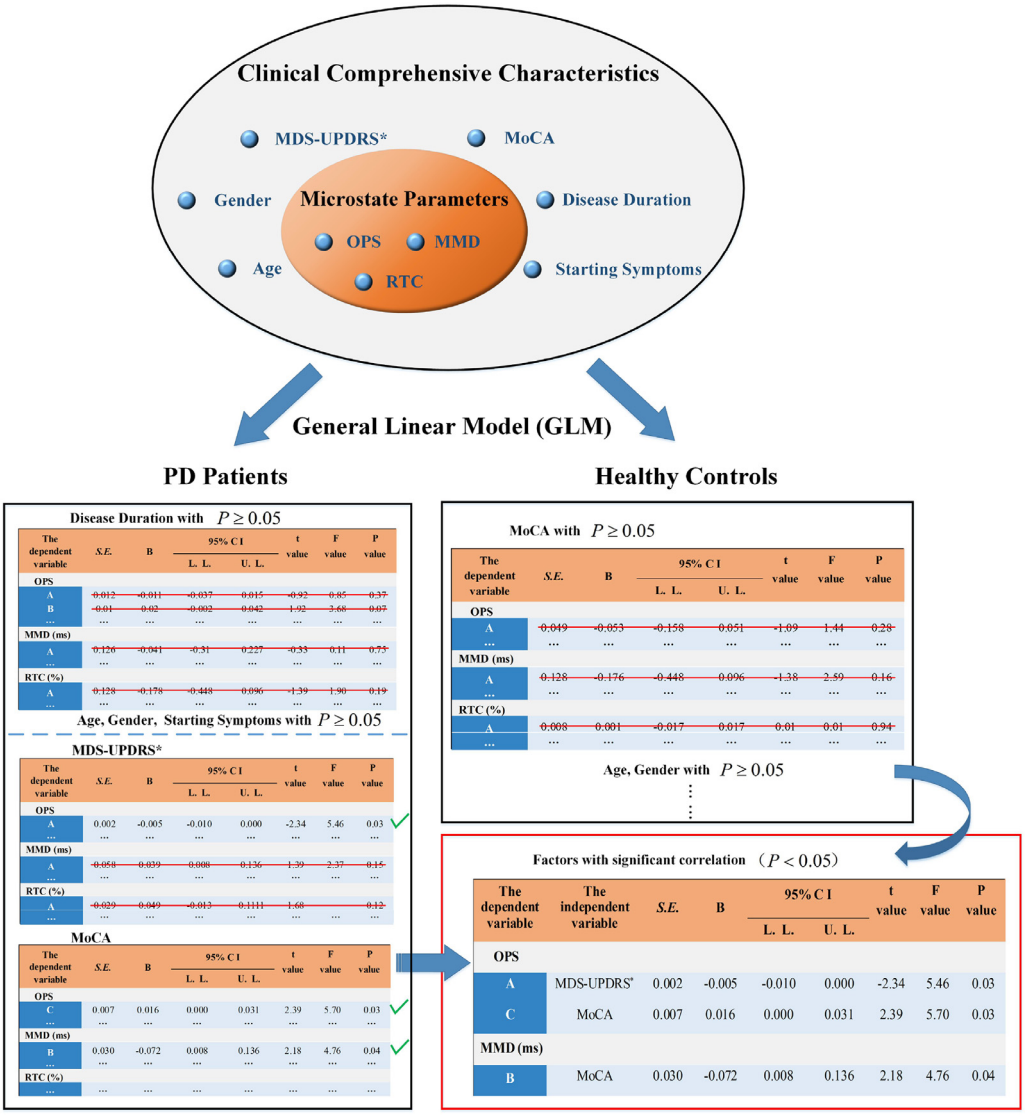

Fig. 5. Significance test of correlation between microstate parameters and all influencing factors in both PD group and control group. General Linear Model (GLM) is performed for significant correlation detection. Significant correlations (P < 0.05) are circled with red dashed wireframe. MDS-UPDRS, Movement Disorder Society-Sponsored Revision of the Unified Parkinson's Disease Rating Scale; MDS-UPDRS*, The Third Part of MDS-UPDRS; MoCA, Montreal Cognitive Assessment.

and the MoCA in PD patients has been found ($R^2 = 0.499$, $\beta = -0.428$, $P = 0.041$). Therefore, we next explored the intuitive and quantifiable linear correlation between microstate parameters and clinical scale scores by analyzing their Spearman's correlation.

3.3.2. *Correlation between microstate parameters and clinical scales*

Fig. 6 shows the results from Spearman's correlation analysis between the third part of the Movement Disorder Society-Sponsored Revision of the Unified Parkinson's Disease Rating Scale (MDS-UPDRS) and all of the microstate characteristic parameters of each microstate class in PD patients with P-values corrected by FDR. There was a negative correlation between OPS of microstate class A and the third part of the MDS-UPDRS in the PD patients ($R = -0.4286$, $P_{FDR} = 0.0413$). However, there were no significant correlation between other characteristic parameters and the third part of MDS-UPDRS score in PD groups with P > 0.05. The lower the third part of MDS-UPDRS's score

Table 3
Clinical correlations between microstate parameters of each microstate class and the clinical characteristics (including disease duration, age, gender, initial symptoms and clinical scales) are calculated by general linear model (GLM).

The dependent variable	The independent variable	*S.E.*	B	95% Confidence Interval		t value	F value	P value
				The lower limit	The upper limit			
OPS								
A	MDS-UPDRS*	0.002	−0.005	−0.010	0.000	−2.34	5.46	0.03
C	MoCA	0.007	0.016	0.000	0.031	2.39	5.70	0.03
MMD (ms)								
B	MoCA	0.030	−0.072	0.008	0.136	2.18	4.76	0.04

S.E., Standard Error; B., Beta, means regression coefficient; MDS-UPDRS, Movement Disorder Society-Sponsored Revision of the Unified Parkinson's Disease Rating Scale; MDS-UPDRS*, The Third Part of MDS-UPDRS; MoCA, Montreal Cognitive Assessment. Significant correlations (P < 0.05) are showed in the table.

Table 4
Clinical correlations between microstate parameters of each microstate class and the clinical scales (after correcting for the confounding effects of disease duration, age, gender, initial symptoms) are calculated by general linear model (GLM) regression.

The dependent variable	The independent variable	R^2	Beta	t value	F value	P value
OPS						
A	MDS-UPDRS*	0.569	−0.380	−2.183	4.547	**0.034**
C	MoCA	0.620	0.500	2.646	7.001	**0.015**
MMD (ms)						
B	MoCA	0.599	−0.428	−2.372	4.717	**0.041**

R^2, the coefficient of determination (range from 0–1). MDS-UPDRS, Movement Disorder Society-Sponsored Revision of the Unified Parkinson's Disease Rating Scale; MDS-UPDRS*, The Third Part of MDS-UPDRS; MoCA, Montreal Cognitive Assessment. Significant correlations ($P < 0.05$) are bold in the table.

is, the more normal the motion function is (Goetz et al., 2010). In other words, within a certain allowable range, the more normal the motor ability of PD patients is, the more occurrence per second of microstate class A. However, it can be seen that the occurrence per second and the mean duration of microstate class A in PD group were observably higher than those in control group (shown in Fig. 4).

Consequently, we further explored the relation between all of the microstate parameters and motor function of microstate class A of PD patients and Fig. 7 is the sketch map. With the gradual deterioration of motor function, the time coverage of microstate class A remained substantially unchanged. This phenomenon corresponded to the opposite trend of occurrence per second and mean duration of microstate class A. Through the overall observation of the three sets of the microstate parameters in class A, we can conclude that the deterioration of motor function in PD is associated with microstate A, and all microstate parameters of class A will increase significantly. Besides, this overall increase is inherently regular, that is, occurrence per second of microstate class A will gradually decrease with the deterioration of motor function but still higher than the normal level, and the corresponding individual level of mean duration of microstate class A will increase accordingly.

Fig. 8 shows the results from Spearman's correlation analysis between the Montreal Cognitive Assessment (MoCA) and characteristic parameters of different microstate classes in PD patients with P-values

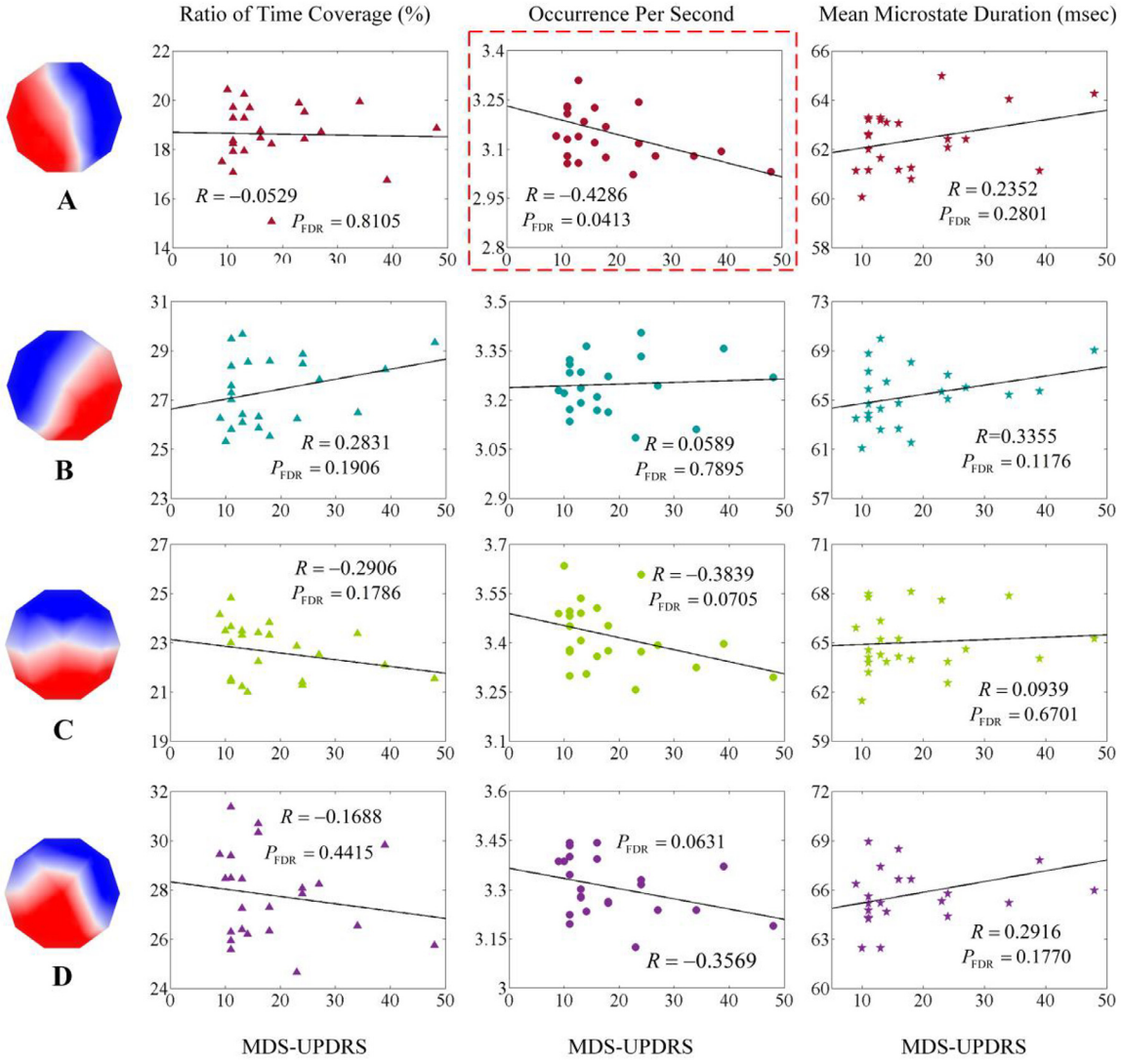

Fig. 6. Clinical the third part of MDS-UPDRS correlations. Spearman correlations between microstate parameters of each microstate class and the third part of MDS-UPDRS. For multiple comparisons, FDR correction is performed for P values. Significant correlations ($P < 0.05$) are circled with red dashed wireframe. Significant correlation between microstate parameter and the score of MDS-UPDRS's third part is indicated by asterisk. MDS-UPDRS, Movement Disorder Society-Sponsored Revision of the Unified Parkinson's Disease Rating Scale.

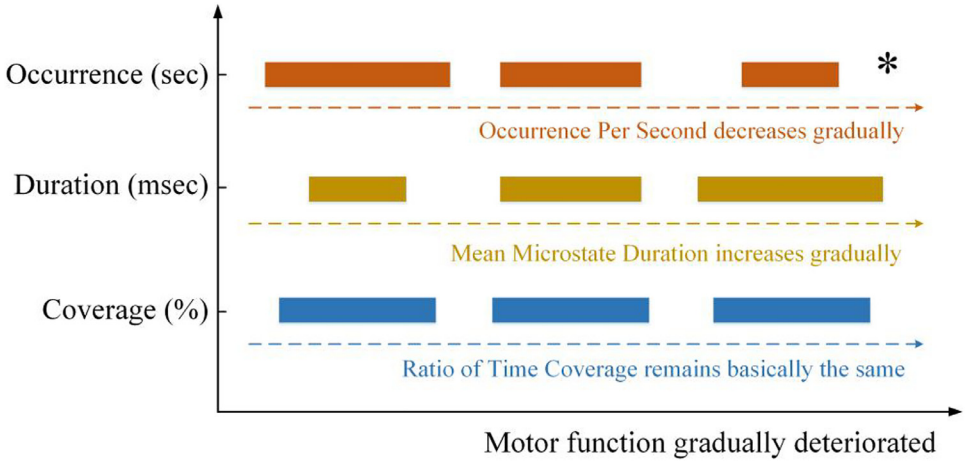

Fig. 7. The sketch map. It shows the relation between the microstate parameters of microstate class A and motor function in PD patients. The extension of the abscissa represents a gradual deterioration of motor function in PD patients. The dotted line with the arrow indicates the change in the value of each microstate parameter. The asterisk means the occurence per second of microstate class A is significantly related to the motor function reflected by the third part of MDS-UPDRS.

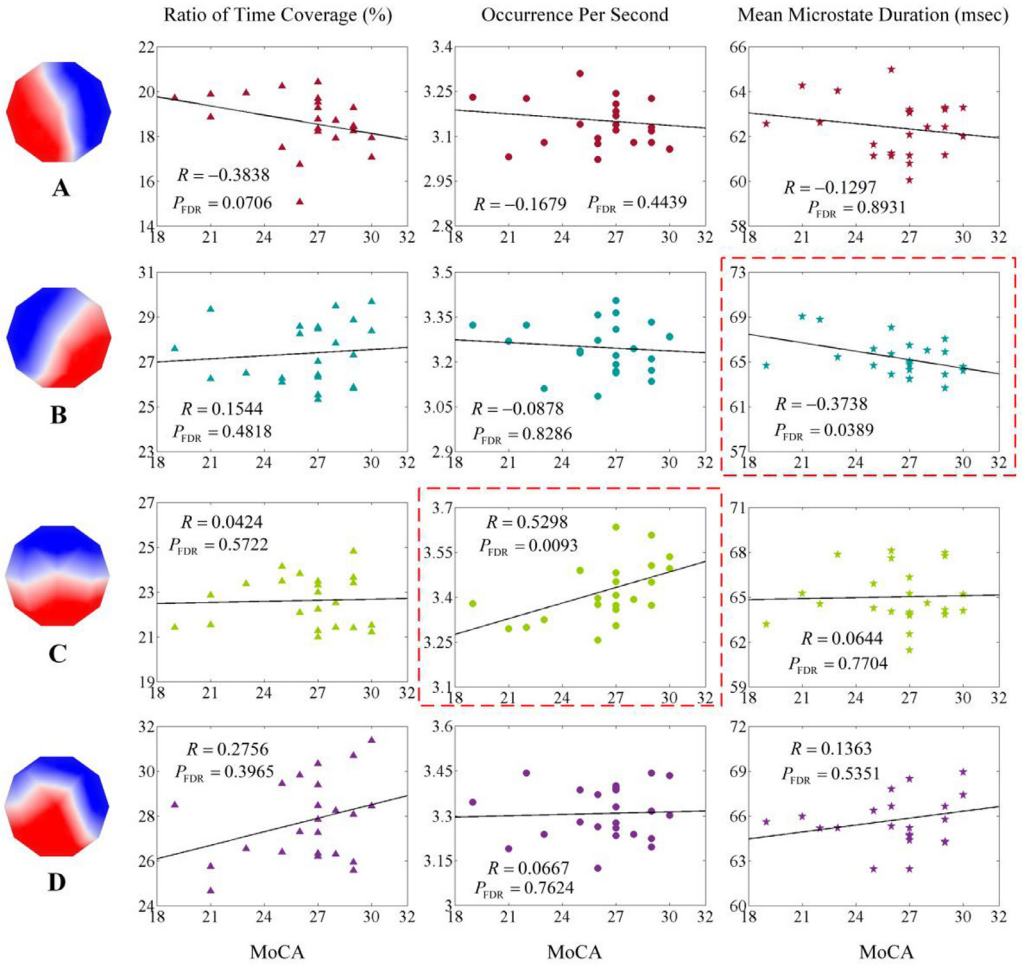

Fig. 8. Clinical MoCA correlations. Spearman correlations between microstate parameters of each microstate class and MoCA. For multiple comparisons, FDR correction is performed for P-value. Significant correlations ($P < 0.05$) are circled with red dashed wireframe. Significant correlations between microstate parameters and MoCA are indicated by asterisk. MoCA, Montreal Cognitive Assessment.

corrected by FDR. There was a significant correlation in both the OPS of the microstate class C (positive correlation with $R = 0.5298$, $P_{FDR} = 0.0093$) and the MMD of the microstate class B (negative correlation with $R = -0.3738$, $P_{FDR} = 0.0389$) with MoCA, and no conspicuous differences in other parameters with $P > 0.05$. When the cognitive performance of the PD patient deteriorates (with a lower MoCA score), the occurrence per second of microstate class C decreases and the mean microstate duration of microstate B increases. This change law corresponds to the result shown in Fig. 4. It can be seen that the closer the values of these two characteristic parameters of the PD group are to the control group, the closer the cognitive ability of PD patients is to the normal level.

4. Discussion

The present study investigated alterations in brain functional state

dynamics in PD patients with tremor and bradykinesia compared to age-matched and gender-matched healthy controls using EEG microstate analysis to ascertain both brain topological structure and temporal characteristics of sub-second brain activity. What's more, the relation between microstate parameters of each EEG microstate class and clinical scales (both motion function (the third part of MDS-UPDRS) and cognitive fatigue (MoCA)) was also explored.

Several studies using simultaneous fMRI and EEG recordings demonstrated that resting state networks (RSNs) assessed by fMRI correlate significantly with the temporal progression of all four EEG microstates (Koenig et al., 1999; Lehmann et al., 2005). Microstate class A is mainly caused by the changes in negative blood-oxygen-level dependence (BOLD) activation of bilateral superior and middle temporal parietal cortex, construed as auditory network (Gschwind et al., 2016; Britz et al., 2010) or sensorimotor (Gschwind et al., 2016; Yuan et al., 2012), while microstate class B exhibited significant correlations with BOLD changes in the striate and extrastriate cortex and the negative BOLD activation in the bilateral occipital cortex, interpreted as visual system (Britz et al., 2010; Yuan et al., 2012; Michel and Koenig, 2017). Microstate class C was related with positive BOLD activation in the bilateral inferior frontal cortices, the dorsal anterior cingulate cortex, and the right insular area, regarded as saliency network (Gschwind et al., 2016; Michel and Koenig, 2017). Microstate D was associated with negative BOLD activation in right lateral ventral and dorsal regions of the frontal cortex and parietal cortex, interpreted as attention network (Gschwind et al., 2016; Michel and Koenig, 2017).

4.1. Microstate spatial topographie

It worth noting that the spatial topography of EEG microstate class D of PD group was variant, whereas no differences existed in the other three EEG microstate classes' topographies. The PD group had almost no topographic map matching the microstate class D of the control group. There are some studies have demonstrated that the patients with schizophrenia have the microstate class D matching the control group, but this kind of microstate has significantly shorter duration and lower occurrence than the normal level, which indicates that schizophrenic patients have similar abnormalities with PD patients. The lack of the typical microstate D in patients with schizophrenic is due to the lack of dopaminergic neurons up to a certain point (Johan et al., 2018). Relatedly, progressive degeneration of dopaminergic neurons in the substantia nigra is associated with the common motor symptoms of tremor, and bradykinesia in PD patients (Kalia, 2015), meanwhile literature (Serrano et al., 2018) indicates that the typical microstate class D matching the control group occurs in PD patients treated with dopamine. Therefore, we can conclude that the deletion of typical microstate class D can be used as one of the early auxiliary diagnostic criteria for PD. The peculiar microstate class D in PD patients in our study showing a strong activation in the dorsal anterior cingulate cortex extending to the superior frontal gyrus is similar as the microstate class F in the literature (Custo et al., 2017). We can assume that microstate class D in PD group is a kind of character state caused of the dopaminergic deficit.

4.2. Microstate temporal characteristics

4.2.1. Correlation between microstate temporal parameters and motor function

From the findings of recent studies, the patients with PD present higher frequency of auditory alterations as a consequence of dopaminergic deficit (Iwaki et al., 2015; Lamas et al., 2017; Toro et al., 2015; Wang et al., 2014; Garrett et al., 2011). As mentioned above, microstate class A is the area implicated in auditory processing network and these clinical features exactly confirm the significant increase of the occurrence of microstate class A in this paper. Besides, individuals with schizophrenia have a higher RTC of microstate class A caused of dopaminergic deficit (Koenig et al., 1999; Lehmann et al., 2005) and larger duration of microstate class A has been reported in PD patients (Serrano et al., 2018). These phenomena are consistent with the temporal characteristics of microstate class A in PD group in this paper, so we can suppose that the temporal abnormalities of microstate class A can be represented as a predictor of PD. Further more, the OPS of microstate class A in PD group was negatively correlated with the third part of MDS-UPDRS's scores, indicating that PD patients' motion function tended to be normal when the OPS of microstate class A was relatively increased.

4.2.2. Correlation between microstate temporal parameters and cognitive level

In a recent study, the longer duration of microstate class B has been identified to be related to cognitive fatigue in the patients with multiple sclerosis (Gschwind et al., 2016), and it could be connected with our present results that as the level of cognition increased, the mean duration of microstate class B gradually decreases to the normal level. So it is reasonable that the significant increased duration of microstate class B is related to the cognitive fatigue presented by PD patients. On the other hand, the coverage of the class B is also observably increased in patients with PD. As we have found the same phenomenon in patients with schizophrenia (Michel and Koenig, 2017), it can be assumed that the increased coverage of microstate B is affected by the combined effects of dopamine deficit and cognitive fatigue in PD patients.

Lower RTC and OPS of microstate class C in PD patients compared to the controls were also demonstrated in the present study. Besides, the positive correlation between MoCA score and OPS indicates that OPS of microstate class C can reflect the cognitive level of PD patients. What's more, the mean duration in microstate class C is decreased compared to normal controls. It can be assuming that the duration and frequency of occurrence are relatively reduced, so the overall coverage is also significantly lower than normal. In a previous study (Mitsuru et al., 2011), the reduction of the OPS of microstate class C relates to the obstacle of the cognitive fatigue and the decreased resting state activity in saliency network regions is due to the lower coverage of class C. Therefore, we can infer that there is a certain decrease in resting state activity in the bilateral inferior frontal cortices, the dorsal anterior cingulate cortex of PD patients, and our results can also indicate that the C state can reflect the cognitive level of PD patients. The present results also suggest that multiple resting state networks are contributing to the configuration of electrical field for microstate class C in the patients with PD, which may reveal abnormal brain dynamics during resting state.

4.3. Limitations

The present study has some limitations. Patients with PD have different mechanisms of tremor and bradykinesia. After striatum dopaminergic system damage, many basal ganglia produce synchronized β wave tremors (Delong, 1990). This is associated with bradykinesia in Parkinson's disease, whereas the symptoms of tremor are not strictly related (Delong, 1990). Symptoms of tremor may be caused by a compensatory mechanism of neurons after the onset of bradykinesia (Marsden, 1984). In addition, the injury of different mechanisms is widely connected between motor and consciousness cortex and cerebellum, which is related to brain dysfunction (Timmermann et al., 2003). Therefore, it is hoped that the dynamic changes of brain activity of the two can be distinguished through EEG microstate analysis, which is conducive to revealing physiological markers corresponding to different symptoms.

We have analyzed the topological maps and the temporal parameters of the microstates of PD patients with tremor and PD patients with bradykinesia, but there were no significant differences between the groups. That's probably caused of the relatively small number of PD patients with one of the symptoms included in the analysis. A larger number of subjects with one of the clinical symptoms and using a larger number of channels to obtain the EEG signals would have produced

more detailed results. Further work will be required to clarify the differences between PD patients with tremor and PD patients with bradykinesia.

5. Conclusions

Resting-state EEG microstate analysis can assess whether transiently stable, sub-second functional states of large-scale brain networks are abnormal, and abnormalities in these functional states are often associated with several neuropsychiatric disorders. In our present research, microstate analysis was used to evaluate the spatiotemporal characteristic markers of brain dysfunction in patients with PD at an early unmedicated condition and the relation between brain dynamics changes and clinical symptoms, such as motor function impairment and cognitive impairments caused by PD pathology was explained. Results revealed that the brain of early-stage PD can be characterized by unique spatial microstates different from healthy controls, which may be related to the brain dysfunction in PD. In addition, the drug-free patients may also show abnormal brain dynamics revealed by the regular changes of temporal microstate features in early PD. Interestingly, such temporal dynamics in microstates are correlated with motor function and cognition of the subjects. The obtained results may deepen our understanding of the brain dysfunction caused by PD, and obtain some quantifiable signatures to provide an auxiliary reference for the early diagnosis of PD. In addition, This study will provide a reference for future research on the mechanism of PD and the pathology of motor and non-motor symptoms.

CRediT authorship contribution statement

Chunguang Chu: Conceptualization, Methodology, Software, Formal analysis, Writing - original draft, Writing - review & editing. **Xing Wang:** Investigation, Resources, Data curation, Software, Writing - original draft. **Lihui Cai:** Writing - original draft, Writing - review & editing. **Lei Zhang:** Resources. **Jiang Wang:** Supervision, Funding acquisition. **Chen Liu:** Supervision, Project administration, Funding acquisition. **Xiaodong Zhu:** Supervision, Project administration, Funding acquisition.

Acknowledgments

Chunguang Chu and Xing Wang are the first author in parallel. The collection and sharing of data for this study were done by Xing Wang, and the processing and analysis of data were completed by Chunguang Chu. The two authors have an equally important contribution to this research. This work was supported by Natural Science Foundation of Tianjin, China, under grant 17JCQNJC00800, National Natural Science Foundation of China under grant 61701336 and Science & Technology Development Fund of Tianjin Education Commissionfor Higher Education under grants 2017ZD10.

References

Berardelli, A., 2001. Pathophysiology of bradykinesia in Parkinson's disease. Brain 124 (11), 2131–2146.
Brandeis, D., Lehmann, D., 1989. Segments of event-related potential map series reveal landscape changes with visual attention and subjective contours. Electroencephalogr. Clin. Neurophysiol. 73 (6), 0–519.
Britz, J., Ville, D.V.D., Michel, C.M., 2010. BOLD correlates of EEG topography reveal rapid resting-state network dynamics. Neuroimage 52 (4), 1162–1170.
Brodbeck, V., Kuhn, A., Wegner, F.V., et al., 2012. EEG microstates of wakefulness and NREM sleep. Neuroimage 62 (3), 2129–2139.
Chu, C., Wang, J., Wang, R., et al., 2018. Complexity analysis of EEG in AD patients with fractional permutation entropy. The 37th Chinese Control Conference 0.
Custo, A., Van, D.V.D., Wells, W.M., et al., 2017. Electroencephalographic resting-state networks: source localization of microstates. Brain Connect.
Deco, G., Jirsa, V.K., Mcintosh, A.R., 2011. Emerging concepts for the dynamical organization of resting-state activity in the brain. Nat. Rev. Neurosci. 12 (1), 43–56.
Delong, M.R., 1990. Primate models of movement disorders of basal ganglia origin. Trends Neurosci. 13.
Dickson, D.W., 2017. Neuropathology of Parkinson disease. Parkinsonism. Relat. Disord. 46.
Gandal, M.J., Edgar, J.C., Klook, K., et al., 2012. Gamma synchrony: towards a translational biomarker for the treatment-resistant symptoms of schizophrenia. Neuropharmacology 62 (3), 1504–1518.
Garrett, A.R., Robertson, D., Sellick, P.M., 2011. The actions of dopamine receptors in the guinea Pig cochlea. Audiol. Neurotol. 16 (3), 145–157.
Garrett, D.D., Samanezlarkin, G.R., Lindenberger, U., et al., 2013. Moment-to-moment brain signal variability: a next frontier in human brain mapping? Neurosci. Biobehav. Rev. 37 (4), 610–624.
Goetz, C.G., Fahn, S., Martinez-Martin, P., et al., 2010. Movement disorder society-sponsored revision of the unified Parkinson's disease rating scale (MDS-UPDRS): process, format, and clinimetric testing plan. Mov. Disord. 23 (15), 2129–2170.
Gschwind, M., Hardmeier, M., Dimitri, V.D.V., et al., 2016. Fluctuations of spontaneous EEG topographies predict disease state in relapsing-remitting multiple sclerosis. NeuroImage 12, 466–477.
Han, C.X., Wang, J., Yi, G.S., et al., 2013. Investigation of EEG abnormalities in the early stage of Parkinson's disease. Cogn. Neurodyn. 7 (4), 351–359.
Iwaki, H., Nishikawa, N., Nagai, M., et al., 2015. Pharmacokinetics of levodopa/benserazide versus levodopa/carbidopa in healthy subjects and patients with Parkinson's disease. Neurol. Clin. Neurosci. 3 (2), 68–73.
Jankovic, J., 2008. Parkinson's disease and movement disorders. Lancet Neurol. 7 (1), 9–11.
Johan, V.D.B.W., Palic, S., Köhler, I., et al., 2018. Access to the CNS: biomarker strategies for dopaminergic treatments. Pharm. Res. 35 (3), 64.
Kalia, L.V., Lang, A.E., 2015. Parkinson's disease. Lancet 386 (9996), 896–912.
Kannan, R., Przekwas, A., 2011. A computational model to detect and quantify a primary blast lung injury using near-infrared optical tomography. Int. J. Numer. Method Biomed. Eng. 27 (1), 13–28.
Kannan, R., Przekwas, A., 2012. A near-infrared spectroscopy computational model for cerebral hemodynamics. Int. J. Numer. Method Biomed. Eng. 28 (11), 1093–1106.
Khanna, A., Pascual-Leone, A., Michel, C.M., et al., 2015. Microstates in resting-state EEG: current status and future directions. Neurosci. Biobehav. Rev. 49, 105–113.
Koenig, T., Kochi, K., Lehmann, D., 1998. Event-related electric microstates of the brain differ between words with visual and abstract meaning. Electroencephalogr. Clin. Neurophysiol. 106 (6), 535–546.
Koenig, T., Kottlow, M., Stein, M., Melie-Garcı´a, L., 2011. Ragu: a free tool for the analysis of EEG and MEG event-related scalp field data using global randomization statistics. Comput. Intell. Neurosci. 2011, 1–14.
Koenig, T., Lehmann, D., Merlo, M.C.G., et al., 1999. A deviant EEG brain microstate in acute, neuroleptic-naive schizophrenics at rest. Eur. Arch. Psychiatry Clin. Neurosci. 249 (4), 205–211.
Koenig, T., Pascualmarqui, R.D., 2009. Electrical neuroimaging: multichannel frequency and time-frequency analysis[M]. Electr. Neuroimag.
Koenig, T., Prichep, L., Lehmann, D., et al., 2002. Millisecond by millisecond, year by year: normative EEG microstates and developmental stages. Neuroimage 16 (1), 41–48.
Lamas, V., Juiz, J.M., Merchán, M.A., 2017. Ablation of the auditory cortex results in changes in the expression of neurotransmission-related mRNAs in the cochlea. Hear. Res. 346, 71–80 Complete.
Lehmann, D., Faber, P.L., Galderisi, S., et al., 2005. EEG microstate duration and syntax in acute, medication-na?ve, first-episode schizophrenia: a multi-center study. Psychiatry Res. 138 (2), 141–156.
Lehmann, D., Ozaki, H., Pal, I., 1987. EEG alpha map series: brain micro-states by space-oriented adaptive segmentation. Electroencephalogr. Clin. Neurophysiol. 67 (3), 0–288.
Lehmann, D., Pascual-Marqui, R.D., Strik, W.K., et al., 2010. Core networks for visual-concrete and abstract thought content: a brain electric microstate analysis. Neuroimage 49 (1), 1073–1079.
Marsden, C.D., 1984. Origins of normal and patholgical tremor. Movement Disorders: Tremor. Palgrave Macmillan, UK.
Menendez, R.G.D.P., Murray, M.M., Michel, C.M., et al., 2004. Electrical neuroimaging based on biophysical constraints. Neuroimage 21 (2), 527–539.
Michel, C.M., Koenig, T., 2017. EEG microstates as a tool for studying the temporal dynamics of whole-brain neuronal networks: a review. Neuroimage S105381191731008X.
Milz, P., Faber, P.L., Lehmann, D., et al., 2015. The functional significance of EEG microstates—Associations with modalities of thinking. Neuroimage 125.
Mitsuru, K., Koenig, T., Munesue, T., et al., 2011. EEG microstate analysis in drug-naive patients with panic disorder. PLoS ONE 6 (7), e22912.
Murray, M.M., Brunet, D., Michel, C.M., 2008. Topographic ERP analyses: a step-by-step tutorial review. Brain Topogr. 20 (4), 249–264.
Rigas, G., Tzallas, A.T., Tsalikakis, D.G., 2009. Real-time quantification of resting tremor in the Parkinson's disease[C]// international conference of the IEEE engineering in medicine & biology society. Conf Proc IEEE Eng Med Biol Soc.
Schlegel, F., Lehmann, D., Faber, P.L., et al., 2012. EEG microstates during resting represent personality differences. Brain Topogr. 25 (1), 20–26.
Schumacher, J., Peraza, L., Firbank, M., et al., 2019. Dysfunctional brain dynamics and their origin in Lewy body dementia. Brain 142 (6), 1767–1782.
Schwingenschuh, P., Ruge, D., Edwards, M.J., et al., 2010. Distinguishing SWEDDs patients with asymmetric resting tremor from Parkinson"s disease: a clinical and electrophysiological study. Mov. Disord. 25 (5), 560–569.
Serrano, J.I., Castillo, del, Dolores, M., Verónica, C., et al., 2018. EEG microstates change in response to increase in dopaminergic stimulation in typical Parkinson's disease patients. Front. Neurosci. 12.

Skrandies, W., 1989. Data reduction of multichannel fields: global field power and principal component analysis. Brain Topogr. 2 (1–2), 73–80.
Timmermann L., Gross J., Dirks M., et al, 2003. The cerebral oscillatory network of parkinsonian resting tremor. Brain. Pt.1 (Pt.1).
Toro, C., Trapani, J.G., Pacentine, I., et al., 2015. Dopamine modulates the activity of sensory hair cells. J. Neurosci. 35 (50), 16494–16503.
VallsSolé, J., Valldeoriola, F., 2002. Neurophysiological correlate of clinical signs in Parkinson's disease. Clin. Neurophysiol. 113 (6), 792–805.
Van, D.V.D., Britz, J., Michel, C.M., 2010. EEG microstate sequences in healthy humans at rest reveal scale-free dynamics. Proceed. Natl. Acad. Sci. 107 (42), 18179–18184.
Wang, L., Li, J., Yu, L., et al., 2014. Regulation of dopamine D2 receptors in the guinea pig cochlea. Acta Otolaryngol. 134 (7), 738–743.
Wang, R., Wang, J., Li, S., et al., 2015. Multiple feature extraction and classification of electroencephalograph signal for Alzheimers" with spectrum and bispectrum. Chaos 25 (1), 013110.
Yuan, H., Zotev, V., Phillips, R., et al., 2012. Spatiotemporal dynamics of the brain at rest — exploring EEG microstates as electrophysiological signatures of bold resting state networks. Neuroimage 60 (4), 2062–2072.
Zalesky, A., Fornito, A., Cocchi, L., et al., 2014. Time-resolved resting-state brain networks. Proceed. Natl. Acad. Sci. 28, 10341–10346 In press.